On relativistic space charge limited current in planar, cylindrical, and spherical diodes

A. D. Greenwood,[1] J. F. Hammond,[1] P. Zhang,[2] and Y. Y. Lau[2]
[1]Air Force Research Laboratory, Directed Energy Directorate, Kirtland AFB, New Mexico 87117-5776, USA
[2]Department of Nuclear Engineering and Radiological Sciences, University of Michigan, Ann Arbor, Michigan 48109-2104, USA

(Received 11 March 2016; accepted 14 June 2016; published online 1 July 2016)

This paper revisits the relativistic limiting current in planar, cylindrical, and spherical diodes, with alternative analytic and numerical treatments which are easy to implement. Convenient, approximate expressions for the limited current are presented for gap voltages up to 10 MV. They are accurate to within 1% for planar diode, and to within 4% for both cylindrical and spherical diode in the range $10^{-5} < r_c/r_a < 500$, where r_a and r_c are, respectively, the anode and cathode radius. *Published by AIP Publishing.* [http://dx.doi.org/10.1063/1.4954827]

I. INTRODUCTION

Space charge limited current has been extensively studied, beginning with the work of Child, Langmuir, and Blodgett.[1–4] Child and Langmuir (CL) independently found a closed form expression for the space charge limited current in a planar diode.[1,2] Langmuir and Blodgett (LB) extended this work to cylindrical and spherical geometries by separating the geometry effects from the voltage and deriving a differential equation for the geometry.[3,4]

The original works by Child, Langmuir, and Blodgett[1–4] adopt a non-relativistic treatment. An early relativistic theory of planar, cylindrical, and spherical diodes was given by Acton in 1957.[5] Acton's paper is largely forgotten now, probably in part due to the limited range of validity in its series solution. Later works on the relativistic planar diode include the oft-cited paper by Jory and Trivelpiece,[6] and the later work by Zhang *et al.*,[7] which includes a relatively simple scaling law. Zhang *et al.*[7] and Chen *et al.*[8] treat the relativistic cylindrical diode, but not the spherical diode. For a relativistic treatment of the spherical diode, reference may be made to Chetvertkov[9] and Belkin *et al.*[10] None of the above references include a convenient formula for the relativistic spherical or cylindrical diode. In addition, Pierce's classical converging gun design was based on the tabulated solution of the non-relativistic spherical diode by Langmuir and Blodgett;[4] here we present a novel, simple scaling law for spherical diodes which is valid up to 10 MV in diode voltage.

The LB theory for the spherical and cylindrical diodes contains a geometrical factor α and β, respectively. These geometrical factors are given in tabulated form in the range $3 \times 10^{-5} < r_c/r_a < 500$, where r_a and r_c are, respectively, the anode and cathode radius.[3,4] Recently, Zhu *et al.*[11] provided a fitting formula for α and β that is accurate to within 5% over the above range of r_c/r_a. Here, we combine the techniques of Zhang *et al.*[7] and Zhu *et al.*[11] to propose fitting formulas for the cylindrical diode [Eqs. (29) and (32)] and for the spherical diode [Eqs. (36) and (39)], for gap voltages up to 10 MV, and $10^{-5} < r_c/r_a < 500$. For completeness, we include the fitting formula of Zhang *et al.*[7] for the relativistic planar diode [Eq. (28)]. Some extensions of the classical diode theory may be found in Refs. 12–15.

In Section II, we express the limiting current in a relativistic planar diode in terms of the hypergeometric function, which readily reduces to the classical CL law in the non-relativistic limits. In Section III, we present two numerical schemes to solve for the relativistic cylindrical and spherical limiting current. The first method employs a Lagrangian formulation. The second method employs a change of variables for the Poisson equation which overcome a numerical singularity near the cathode. Both methods allow ready numerical solutions and we have confirmed that they yield identical numerical results. The numerical results are fitted into simple, ready to use formulas in Section IV.

II. PLANAR DIODE

First, an alternate relativistic solution of the one-dimensional planar diode is presented. This new solution has the advantage of being closed form and reducing to the classical CL solution in a simple manner.[6,14] Consider the planar diode geometry shown in Fig. 1. Denote the cathode location as z_c and the anode location as z_a. Referring to Fig. 1, either $z_c = z_1$ and $z_a = z_2$, or $z_c = z_2$ and $z_a = z_1$. Further, the separation between the plates is $d = z_2 - z_1$. Let the cathode be at a potential of $\Phi = 0$ V, and the anode be at a potential of $\Phi = V_0 > 0$. The space charge limit implies that, at the cathode, $d\Phi/dz = 0$. A relativistic electron accelerated through a potential, Φ, attains a kinetic energy

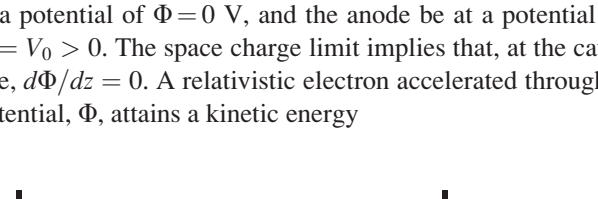

FIG. 1. Geometry of a one-dimensional, planar diode.

$$(\gamma - 1)mc^2 = \Phi e, \tag{1}$$

where m is the electron rest mass, c is the speed of light, and e is the absolute value of the electron charge. Substituting the definition $\gamma = (1 - (v/c)^2)^{-1/2}$, it can be shown that velocity of the electrons is

$$v = \pm c \frac{\sqrt{\frac{\Phi e}{mc^2}\left(\frac{\Phi e}{mc^2} + 2\right)}}{\frac{\Phi e}{mc^2} + 1}, \tag{2}$$

where the sign is chosen based on the direction of motion. Assuming dependence on z only, and substituting $\mathbf{E} = -\nabla\Phi$ into Gauss's law yields Poisson's equation

$$\frac{d^2\Phi}{dz^2} = -\frac{\rho}{\epsilon_0}. \tag{3}$$

The current density in the z direction in A/m^2 is given by

$$J_{\text{planar}} = \rho v, \tag{4}$$

and substituting into Poisson's equation and using Eq. (2) gives

$$\frac{d^2\Phi}{dz^2} = \frac{|J_{\text{planar}}|\left(\frac{\Phi e}{mc^2} + 1\right)}{\epsilon_0 c\sqrt{\frac{\Phi e}{mc^2}\left(\frac{\Phi e}{mc^2} + 2\right)}}, \tag{5}$$

with boundary conditions

$$\Phi(z = z_c) = 0, \tag{6}$$

$$\left.\frac{d\Phi}{dz}\right|_{z=z_c} = 0. \tag{7}$$

Following the procedure in Ref. 14, multiply Eq. (5) by $d\Phi/dz$ to allow analytic integration, giving

$$\left(\frac{d\Phi}{dz}\right)^2 = \frac{2mc|J_{\text{planar}}|\sqrt{\frac{\Phi e}{mc^2}\left(\frac{\Phi e}{mc^2} + 2\right)}}{e\epsilon_0} + C_1. \tag{8}$$

Examining the boundary conditions shows that the constant of integration, $C_1 = 0$. Rearranging Eq. (8) and taking the square root gives

$$\left[\frac{\Phi e}{mc^2}\left(\frac{\Phi e}{mc^2} + 2\right)\right]^{-1/4}\frac{d\Phi}{dz} = \sqrt{\frac{2mc|J_{\text{planar}}|}{e\epsilon_0}}, \tag{9}$$

which can again be integrated, yielding

$$\frac{2(2\Phi)^{3/4}}{3(emc^2)^{1/4}}\,{}_2F_1\left(\frac{1}{4},\frac{3}{4};\frac{7}{4};-\frac{\Phi e}{2mc^2}\right) = \sqrt{\frac{2|J_{\text{planar}}|}{e\epsilon_0 c}}(z - z_c), \tag{10}$$

where the constant of integration is evaluated to enforce $\Phi(z_c) = 0$ and ${}_2F_1$ denotes a hypergeometric function. Evaluating at $z = z_a$ and solving for the current density gives

$$|J_{\text{planar}}| = \frac{4}{9}\epsilon_0\sqrt{\frac{2e}{m}}\frac{V_0^{3/2}}{d^2}\left[{}_2F_1\left(\frac{1}{4},\frac{3}{4};\frac{7}{4};-\frac{V_0 e}{2mc^2}\right)\right]^2. \tag{11}$$

Examining Eq. (11) reveals it is identical to the classical CL expression multiplied by the square of the hypergeometric function. Further, the hypergeometric function approaches 1 as $V_0 e/(2mc^2)$ becomes small. Thus, Eq. (11) reduces to the classical expression at small voltage, and the square of the hypergeometric function provides the necessary relativistic correction. For $V_0 e > 2mc^2$, the infinite series for the hypergeometric function in Eq. (11) is divergent; its analytic continuation may be used.

III. CYLINDRICAL AND SPHERICAL DIODE

To derive a convenient equation to integrate numerically to find the current in a coaxial cylinder or concentric sphere geometry, first consider the cross-section shown in Fig. 2. Similar to the planar diode, denote the cathode radius r_c and the anode radius r_a. Referring to Fig. 2, either $r_c = r_1$ and $r_a = r_2$, or $r_c = r_2$ and $r_a = r_1$. Also similar to the planar diode, let the cathode be at a potential of $\Phi = 0$ V, and the anode be at a potential of $\Phi = V_0 > 0$. The space charge limit implies that, at the cathode, $d\Phi/dr = 0$.

Langmuir and Blodgett[3,4] considered this problem in a classical (non-relativistic) sense by separating the effect of the geometry from the voltage and deriving a differential equation for the geometry parameter. In the fully relativistic equations, the geometry effect is no longer separable. In the derivation that follows, the coaxial cylinder equations are on the left and the concentric sphere equations on the right.

Define J_{cyl} to be the cylindrical radial current per unit axial length in A/m and I_{sph} to be the total spherical radial current in A. Then, the differential equations governing the diode currents are

$$\frac{d}{dr}\left(r\frac{d\Phi}{dr}\right) = -\frac{J_{\text{cyl}}}{2\pi\epsilon_0 v}, \quad \frac{d}{dr}\left(r^2\frac{d\Phi}{dr}\right) = -\frac{I_{\text{sph}}}{4\pi\epsilon_0 v}. \tag{12}$$

Substituting Eq. (2) and noting that both Φ and its first derivative are zero at the cathode reveals the second derivative of Φ must be approaching infinity at the cathode. This complicates

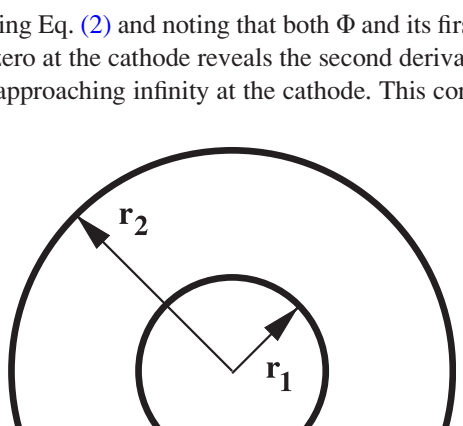

FIG. 2. Cross-section of the coaxial cylinder or concentric sphere geometry.

the numerical integration of these equations. Two methods of dealing with this difficulty are presented below.

A. Method 1: Use of Lagrangian variable, *t*

Define t to be the time in transit across gap, such that $t=0$ is the time a given electron is born at the cathode. By the chain rule

$$\frac{d}{dt}(*) = \frac{dr}{dt}\frac{d}{dr}(*) = v\frac{d}{dr}(*). \tag{13}$$

Thus, Eq. (12) becomes

$$\frac{d}{dt}\left(r\frac{d\Phi}{dr}\right) = -\frac{J_{\rm cyl}}{2\pi\epsilon_0}, \quad \frac{d}{dt}\left(r^2\frac{d\Phi}{dr}\right) = -\frac{I_{\rm sph}}{4\pi\epsilon_0}. \tag{14}$$

Integrating and noting that the $\frac{d\Phi}{dr}|_{t=0} = 0$ gives

$$\frac{d\Phi}{dr} = -\frac{J_{\rm cyl}t}{2\pi r\epsilon_0}, \quad \frac{d\Phi}{dr} = -\frac{I_{\rm sph}t}{4\pi r^2\epsilon_0}. \tag{15}$$

Again applying the chain rule gives

$$\frac{d\Phi}{dt} = -\frac{J_{\rm cyl}t}{2\pi r\epsilon_0}\frac{dr}{dt}, \quad \frac{d\Phi}{dt} = -\frac{I_{\rm sph}t}{4\pi r^2\epsilon_0}\frac{dr}{dt}. \tag{16}$$

Combining Eq. (16) with the expression for the velocity,

$$v = \frac{dr}{dt} = \pm\frac{c\sqrt{\frac{\Phi e}{mc^2}\left(\frac{\Phi e}{mc^2}+2\right)}}{\frac{\Phi e}{mc^2}+1}, \tag{17}$$

gives a system of equations which can be numerically integrated. Note that the sign in Eq. (17) depends on whether the cathode is outside or inside the anode. These equations can be non-dimensionalized using $\bar{t} = ct/r_c$, $\bar{r} = r/r_c$, $\bar{\Phi} = \Phi e/(mc^2)$, $\bar{J}_{\rm cyl} = \eta J_{\rm cyl} r_c e/(mc^2)$ and $\bar{I}_{\rm sph} = \eta I_{\rm sph} e/(mc^2)$ and noting that $\eta = 1/(\epsilon_0 c)$

$$\begin{bmatrix}\frac{d\bar{\Phi}}{d\bar{t}}\\ \frac{d\bar{r}}{d\bar{t}}\end{bmatrix} = \begin{bmatrix}-\frac{\bar{J}_{\rm cyl}\bar{t}}{2\pi\bar{r}}\frac{d\bar{r}}{d\bar{t}}\\ \pm\frac{\sqrt{\bar{\Phi}(\bar{\Phi}+2)}}{\bar{\Phi}+1}\end{bmatrix}, \quad \begin{bmatrix}\frac{d\bar{\Phi}}{d\bar{t}}\\ \frac{d\bar{r}}{d\bar{t}}\end{bmatrix} = \begin{bmatrix}-\frac{\bar{I}_{\rm sph}\bar{t}}{4\pi\bar{r}^2}\frac{d\bar{r}}{d\bar{t}}\\ \pm\frac{\sqrt{\bar{\Phi}(\bar{\Phi}+2)}}{\bar{\Phi}+1}\end{bmatrix},$$
$$\bar{\Phi}(\bar{t}=0) = 0, \quad \bar{\Phi}(\bar{t}=0) = 0,$$
$$\bar{r}(\bar{t}=0) = 1, \quad \bar{r}(\bar{t}=0) = 1. \tag{18}$$

Given a current density $\bar{J}_{\rm cyl}$ or current $\bar{I}_{\rm sph}$, the equations can be integrated until $\bar{r} = r_a/r_c$ to find the transit time and the anode potential together. The problem of finding the current or current density from the anode potential is discussed in Sec. III C.

B. Method 2: Change of variables

An alternate method is to substitute Eq. (17) into Eq. (12), giving

$$\frac{d}{dr}\left(r\frac{d\Phi}{dr}\right) = \frac{\eta|J_{\rm cyl}|}{2\pi}\frac{\frac{\Phi e}{mc^2}+1}{\sqrt{\frac{\Phi e}{mc^2}\left(\frac{\Phi e}{mc^2}+2\right)}},$$
$$\frac{d}{dr}\left(r^2\frac{d\Phi}{dr}\right) = \frac{\eta|I_{\rm sph}|}{4\pi}\frac{\frac{\Phi e}{mc^2}+1}{\sqrt{\frac{\Phi e}{mc^2}\left(\frac{\Phi e}{mc^2}+2\right)}}, \tag{19}$$

where $\eta = 1/(\epsilon_0 c)$ is used. Similar to the case above, these equations are non-dimensionalized with $\bar{r} = r/r_c$, $\bar{\Phi} = \Phi e/(mc^2)$, $\bar{J}_{\rm cyl} = \eta J_{\rm cyl} r_c e/(mc^2)$, and $\bar{I}_{\rm sph} = \eta I_{\rm sph} e/(mc^2)$

$$\frac{d}{d\bar{r}}\left(\bar{r}\frac{d\bar{\Phi}}{d\bar{r}}\right) = \bar{r}\frac{d^2\bar{\Phi}}{d\bar{r}^2} + \frac{d\bar{\Phi}}{d\bar{r}} = \frac{|\bar{J}_{\rm cyl}|}{2\pi}\frac{\bar{\Phi}+1}{\sqrt{\bar{\Phi}(\bar{\Phi}+2)}},$$
$$\frac{d}{d\bar{r}}\left(\bar{r}^2\frac{d\bar{\Phi}}{d\bar{r}}\right) = \bar{r}^2\frac{d^2\bar{\Phi}}{d\bar{r}^2} + 2\bar{r}\frac{d\bar{\Phi}}{d\bar{r}} = \frac{|\bar{I}_{\rm sph}|}{4\pi}\frac{\bar{\Phi}+1}{\sqrt{\bar{\Phi}(\bar{\Phi}+2)}}. \tag{20}$$

To avoid the singularity in the second derivative at the cathode, the equations can be transformed using $\bar{\Psi} = \bar{\Phi}^{3/2}$

$$\frac{d^2\bar{\Psi}}{d\bar{r}^2} = \frac{3|\bar{J}_{\rm cyl}|}{4\pi\bar{r}}\frac{\bar{\Psi}^{2/3}+1}{\sqrt{\bar{\Psi}^{2/3}+2}} + \frac{1}{3\bar{\Psi}}\left(\frac{d\bar{\Psi}}{d\bar{r}}\right)^2 - \frac{1}{\bar{r}}\frac{d\bar{\Psi}}{d\bar{r}},$$
$$\frac{d^2\bar{\Psi}}{d\bar{r}^2} = \frac{3|\bar{I}_{\rm sph}|}{8\pi\bar{r}^2}\frac{\bar{\Psi}^{2/3}+1}{\sqrt{\bar{\Psi}^{2/3}+2}} + \frac{1}{3\bar{\Psi}}\left(\frac{d\bar{\Psi}}{d\bar{r}}\right)^2 - \frac{2}{\bar{r}}\frac{d\bar{\Psi}}{d\bar{r}},$$
$$\bar{\Psi}(\bar{r}=1) = 0,$$
$$\left.\frac{d\bar{\Psi}}{d\bar{r}}\right|_{\bar{r}=1} = 0,$$
$$\bar{\Psi}\left(\bar{r} = \frac{r_a}{r_c}\right) = \left(\frac{V_0 e}{mc^2}\right)^{3/2}, \tag{21}$$

$d^2\bar{\Psi}/d\bar{r}^2$ approaches a finite limit at the cathode, given by

$$\lim_{\bar{r}\to 1}\frac{d^2\bar{\Psi}}{d\bar{r}^2} = \frac{9|\bar{J}_{\rm cyl}|}{4\pi\sqrt{2}}, \quad \lim_{\bar{r}\to 1}\frac{d^2\bar{\Psi}}{d\bar{r}^2} = \frac{9|\bar{I}_{\rm sph}|}{8\pi\sqrt{2}}. \tag{22}$$

This allows a Taylor series solution for $\bar{\Psi}$ as $\bar{r}$ approaches the cathode ($\bar{r}\to 1$)

$$\bar{\Psi}(\bar{r}) = \frac{9|\bar{J}_{\rm cyl}|}{8\pi\sqrt{2}}(\bar{r}-1)^2, \quad \bar{\Psi}(\bar{r}) = \frac{9|\bar{I}_{\rm sph}|}{16\pi\sqrt{2}}(\bar{r}-1)^2. \tag{23}$$

Additional terms for the Taylor series can be generated by differentiating the equation for $d^2\bar{\Psi}/d\bar{r}^2$ in Eq. (21) with respect to $\bar{r}$ and applying L'Hôpital's rule, a task which is much simpler if it is noted that, in the vicinity of the cathode, $\bar{\Psi}^{2/3} \ll 1$, thus

$$\frac{\bar{\Psi}^{2/3}+1}{\sqrt{\bar{\Psi}^{2/3}+2}} \approx \frac{1}{\sqrt{2}} \quad \text{as} \quad \bar{r}\to 1. \tag{24}$$

For use with packaged numerical ordinary differential equation integrators, Eq. (21) can be converted to a system of first order ordinary differential equations by defining $\bar{\Upsilon} = d\bar{\Psi}/d\bar{r}$

$$\begin{bmatrix} \frac{d\bar{\Psi}}{d\bar{r}} \\ \frac{d\bar{\Upsilon}}{d\bar{r}} \end{bmatrix} = \begin{bmatrix} \bar{\Upsilon} \\ \frac{3|\bar{J}_{\rm cyl}|}{4\pi\bar{r}} \frac{\bar{\Psi}^{2/3}+1}{\sqrt{\bar{\Psi}^{2/3}+2}} + \frac{\bar{\Upsilon}^2}{3\bar{\Psi}} - \frac{\bar{\Upsilon}}{\bar{r}} \end{bmatrix},$$

$$\begin{bmatrix} \frac{d\bar{\Psi}}{d\bar{r}} \\ \frac{d\bar{\Upsilon}}{d\bar{r}} \end{bmatrix} = \begin{bmatrix} \bar{\Upsilon} \\ \frac{3|\bar{I}_{\rm sph}|}{8\pi\bar{r}^2} \frac{\bar{\Psi}^{2/3}+1}{\sqrt{\bar{\Psi}^{2/3}+2}} + \frac{\bar{\Upsilon}^2}{3\bar{\Psi}} - \frac{2\bar{\Upsilon}}{\bar{r}} \end{bmatrix},$$

$$\bar{\Psi}(\bar{r}=1)=0,$$

$$\bar{\Upsilon}(\bar{r}=1)=0,$$

$$\bar{\Psi}\left(\bar{r}=\frac{r_a}{r_c}\right)=\left(\frac{V_0 e}{mc^2}\right)^{3/2}, \tag{25}$$

In this context, the Taylor series approximation near the cathode ($\bar{r} \to 1$) is

$$\begin{bmatrix} \bar{\Psi}(\bar{r}) \\ \bar{\Upsilon}(\bar{r}) \end{bmatrix} = \begin{bmatrix} \frac{9|\bar{J}_{\rm cyl}|(\bar{r}-1)^2}{8\pi\sqrt{2}} \\ \frac{9|\bar{J}_{\rm cyl}|(\bar{r}-1)}{4\pi\sqrt{2}} \end{bmatrix}, \quad \begin{bmatrix} \bar{\Psi}(\bar{r}) \\ \bar{\Upsilon}(\bar{r}) \end{bmatrix} = \begin{bmatrix} \frac{9|\bar{I}_{\rm sph}|(\bar{r}-1)^2}{16\pi\sqrt{2}} \\ \frac{9|\bar{I}_{\rm sph}|(\bar{r}-1)}{8\pi\sqrt{2}} \end{bmatrix}. \tag{26}$$

Note that numerical integrators of ordinary differential equations often encounter difficulty when starting at initial conditions of zero. The Taylor series approximation allows this problem to be avoided by starting the process with finite initial conditions at $\bar{r} = 1 + \delta$, where δ is a small number.

C. Finding the current from the gap voltage

Eq. (18) or (25) is convenient for finding the gap voltage (V_0) given a current density (coaxial cylinders) or current (concentric spheres). Often, the gap voltage is given, and the current density or current is the quantity to determine. For this task, consider Fig. 3 where the current density or current is shown as a function of gap voltage. Also shown are the classical LB[3,4] result and an ultra-relativistic approximation, derived by assuming $\bar{\Phi} \gg 2$ and analytically integrating the resulting approximation to Eq. (20). The ultra-relativistic approximation is thus given by

$$J_{\rm cyl}^{\rm ur} = \frac{2\pi V_0}{\eta r_a[1 - r_c/r_a - (r_c/r_a)\ln(r_a/r_c)]},$$
$$I_{\rm sph}^{\rm ur} = \frac{4\pi V_0}{\eta[r_c/r_a - 1 - \ln(r_c/r_a)]}, \tag{27}$$

where $\bar{V}_0 = V_0 e/(mc^2)$. The point at which the classical LB current crosses the ultra-relativistic current is easily determined. Note that to the left of that point, the classical LB current over estimates the fully relativistic current. Similarly, to the right of that point, the ultra-relativistic current over estimates the fully relativistic current. Thus, starting from an approximation known to over estimate the true result, a bisection algorithm can quickly find the current density or current from the gap voltage with a few numerical integrations of Eq. (18) or (25).

IV. FITTING FORMULAS FOR RELATIVISTIC PLANAR, CYLINDRICAL, AND SPHERICAL DIODES

For a planar diode, Zhang *et al.*[7] derive the approximate solution

$$J_{\rm planar} = \frac{2}{\eta}\frac{mc^2}{ed^2}\frac{\left(\gamma^{2/3}-1\right)^{3/2}}{\left(\sqrt{3}-1\right)\gamma^{-p}+1}, \tag{28}$$

where $\gamma = 1 + eV_0/(mc^2)$ and p is a fitting parameter set to 0.392 in Ref. 7. Note that in Ref. 7, p is denoted α; the notation change to p avoids confusion with the spherical LB geometry factor, which is denoted as α below. Use of Eq. (28) avoids the computation of the hypergeometric function in Eq. (11), and the error for $V_0 < 10$ MV is less than 0.9%, as shown in Fig. 4.

For a cylindrical diode, Zhang *et al.*[7] derived the approximate solution

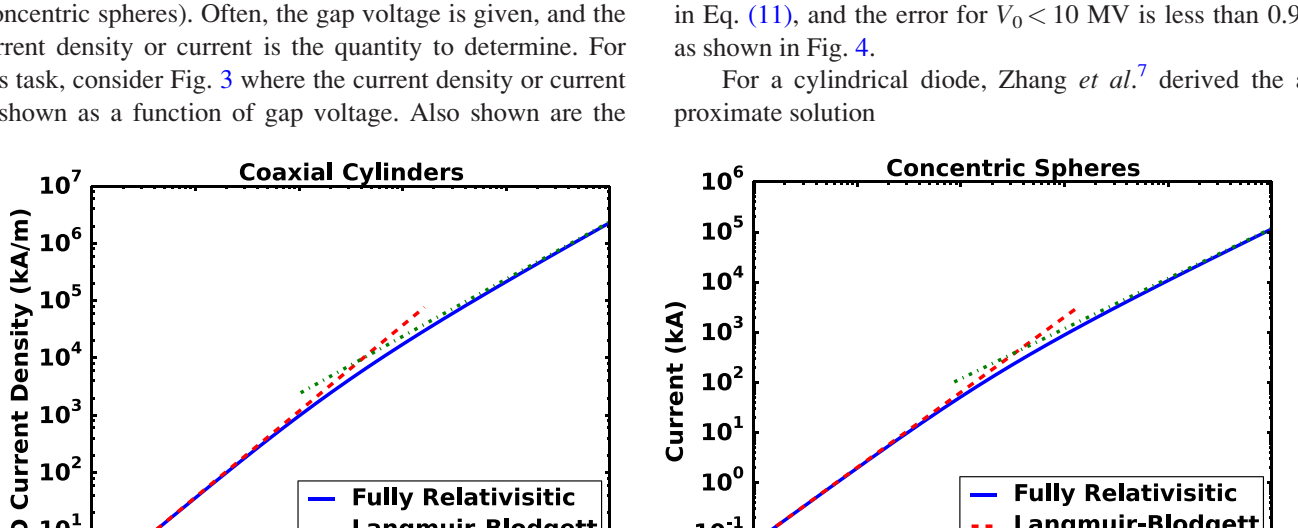

FIG. 3. Current as a function of gap voltage for $r_c = 1.4$ cm and $r_a = 3.3$ cm.

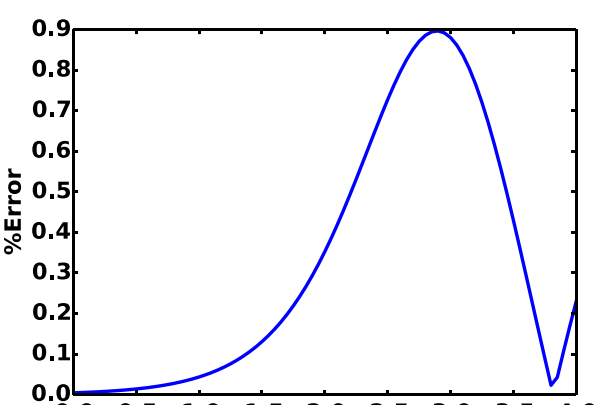

FIG. 4. Plot showing the error of the approximate current solution for a planar diode.

$$J_{\rm cyl} = \frac{2\pi}{\eta}\frac{mc^2}{erA(u)}\frac{\left(\gamma^{2/3}-1\right)^{3/2}}{\left(\frac{\sqrt{3}}{2}\frac{\beta^2(u)}{A(u)}-1\right)\gamma^{-p}+1}, \tag{29}$$

where $u = r_a/r_c$, $A(u) = 1 - u^{-1} - u^{-1}\ln u$, and $\beta^2(u)$ is the LB geometry factor.[3] Comparing to the numerically integrated solution for $V_0 < 10$ MV and $10^{-5} < r_c/r_a < 500$, the error is minimized for $p = 0.384$. For $p = 0.384$, the error is less than 3.9% over the range $V_0 < 10$ MV and $10^{-5} < r_c/r_a < 500$. The error can be lowered to less than 2.4% by using $p = 0.384 + f_1(x,y) + f_2(x,y)$ where $x = \log_{10}(r_c/r_a)$, $y = \log_{10}(V_0/1kV)$, and

$$\begin{aligned} d_1 &= \left(\frac{x+5}{4}\right)^2 + \left(\frac{y-3.3}{2}\right)^2, \\ f_1(x,y) &= \begin{cases} -0.2*(1-d_1) & d_1 < 1 \\ 0 & \text{else}, \end{cases} \end{aligned} \tag{30}$$

$$\begin{aligned} d_2 &= \left(\frac{x-2.7}{2.8}\right)^2 + \left(\frac{y-4.0}{0.6}\right)^2, \\ f_2(x,y) &= \begin{cases} 0.05*(1-d_2) & d_2 < 1 \\ 0 & \text{else}. \end{cases} \end{aligned} \tag{31}$$

Note that $y = \log_{10}(V_0/1kV)$ encounters a singularity as $V_0 \to 0$. However, $d_1 > 1$ and therefore $f_1 = 0$ for all $y < 1.3$, which corresponds to $V_0 < 19.95$ kV, and $d_2 > 1$ and therefore $f_2 = 0$ for all $y < 3.4$, which corresponds to $V_0 < 2.51$ MV. Thus, in the deep non-relativistic limit, y need not be computed. Alternatively, the non-relativistic scaling given in Ref. 11 is valid in this regime. The approximation in Eq. (29) is still difficult to use due to the inclusion of the LB geometry factor $\beta^2(u)$. Its use is simplified by using an approximate geometry factor[11]

$$\beta^2_{\rm approx}(u) = \begin{cases} \dfrac{|u-1|^{1/2}|\ln(u)|^{3/2}}{u\left[1+F_{\rm cyl}(1/u)\right]} & u < 781.07 \\ 1 & \text{else}, \end{cases} \tag{32}$$

where

$$F_{\rm cyl}\left(\frac{r_c}{r_a}\right) = \exp\left[\frac{(s-s_0)(7s+23)(8s-417)}{143742}\right] - 1, \tag{33}$$

$$s = \ln[\ln(1 + r_c/r_a)], \tag{34}$$

$$s_0 = \ln[\ln(2)]. \tag{35}$$

The use of the approximate geometry factor in Eq. (29) increases the maximum error to 4.0%. Plots of the error over the $V_0 < 10$ MV and $10^{-5} < r_c/r_a < 500$ range using both exact and the approximate geometry parameter are shown in Fig. 5.

Following the methodology of Ref. 7 for the spherical case yields

$$I_{\rm sph} = \frac{4\pi}{\eta}\frac{mc^2}{eB(u)}\frac{\left(\gamma^{2/3}-1\right)^{3/2}}{\left(\frac{\sqrt{3}}{2}\frac{\alpha^2(u)}{B(u)}-1\right)\gamma^{-p}+1}, \tag{36}$$

where $B(u) = u^{-1} - 1 - \ln u^{-1}$ and $\alpha^2(u)$ is the LB geometry factor.[4] In this case, a constant value of $p = 0.360$ leads to an error of less than 6.7%. The error can be lowered to less than 3.3% using $p = 0.325 + f_1(x,y) + f_2(x,y)$ where $x = \log_{10}(r_c/r_a)$, $y = \log_{10}(V_0/1\,kV)$, and

$$\begin{aligned} d_1 &= \left(\frac{x+5}{4}\right)^2 + \left(\frac{y-4}{2}\right)^2, \\ f_1(x,y) &= \begin{cases} 0.12*(1-d_1) & d_1 < 1 \\ 0 & \text{else}, \end{cases} \end{aligned} \tag{37}$$

$$\begin{aligned} d_2 &= \left[\frac{(x-2)*\sqrt{3}/2 + (y-5)/2}{4}\right]^2 \\ &\quad + \left[\frac{-(x-2)/2 + (y-5)*\sqrt{3}/2}{2}\right]^2, \\ f_2(x,y) &= \begin{cases} 0.07*(1-d_2) & d_2 < 1 \\ 0 & \text{else}. \end{cases} \end{aligned} \tag{38}$$

Similar to the cylindrical diode case, the singularity of $y = \log_{10}(V_0/1\text{kV})$ as $V_0 \to 0$ can be avoided by noting that $d_1 > 1$ and therefore $f_1 = 0$ for all $y < 2$, which corresponds to $V_0 < 100$ kV, and $d_2 > 1$ and therefore $f_2 = 0$ for all $y < 2.78$, which corresponds to $V_0 < 604$ kV. Thus, y need not be computed in the non-relativistic limit. Alternatively, in the non-relativistic limit, the scaling in Ref. 11 can be used. The use of Eq. (36) can be simplified by using an approximate geometry factor[11]

$$\alpha^2_{\rm approx}(u) = \frac{(u-1)^2}{u^{3/2}\left[1+F_{\rm sph}(1/u)\right]}, \tag{39}$$

where

$$F_{\rm sph}\left(\frac{r_c}{r_a}\right) = \exp\left[\frac{(s-s_0)(9s-37)(4s+143)}{42092}\right] - 1, \tag{40}$$

and s and s_0 are as defined in Eqs. (34) and (35). Use of the approximate geometry parameter results in a maximum error in the current of 3.1%. Plots of the error over the $V_0 < 10$ MV

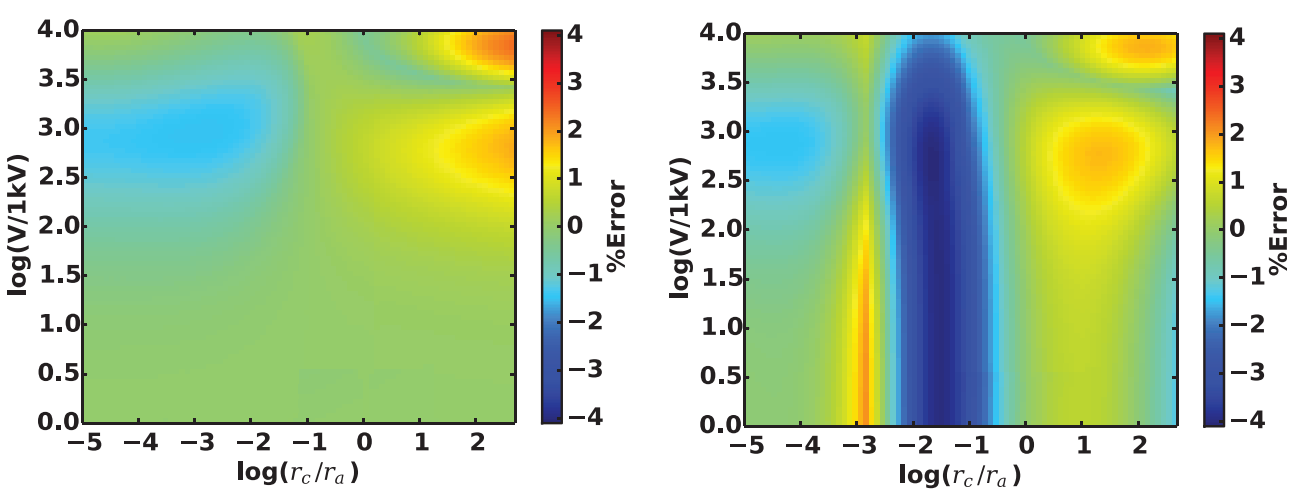

FIG. 5. Plots showing the error of the approximate current solution for a cylindrical diode using (a) the exact and (b) the approximate LB geometry parameter.

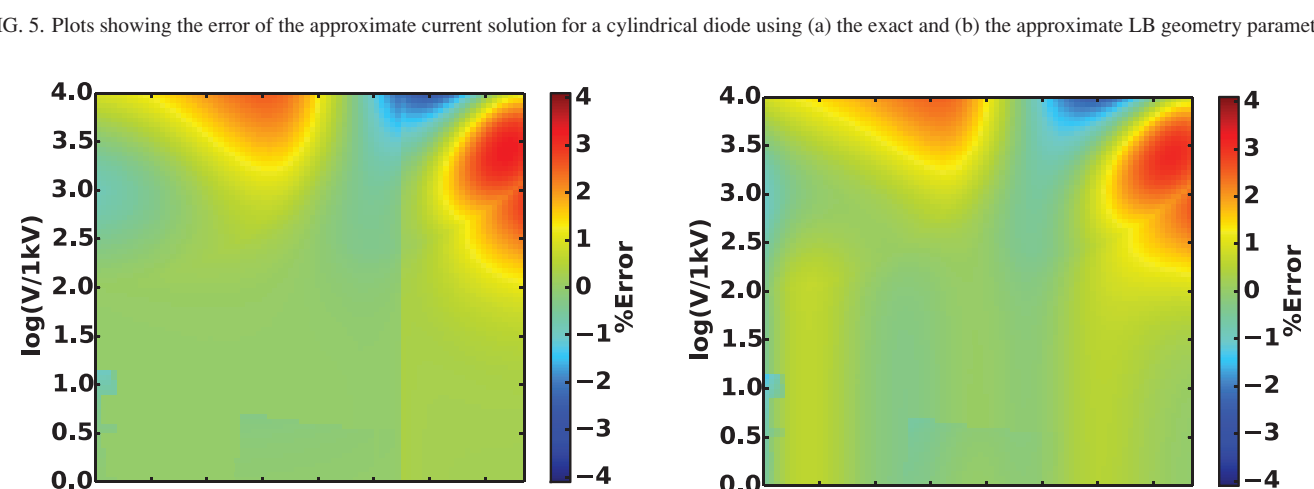

FIG. 6. Plots showing the error of the approximate current solution for a spherical diode using (a) the exact and (b) the approximate LB geometry parameter.

and $10^{-5} < r_c/r_a < 500$ range using both exact and the approximate geometry parameter are shown in Fig. 6.

V. CONCLUSION

Space charge limited current in relativistic diodes is extensively studied. Herein, a relativistically correct solution is presented for a planar diode that reduces to the classical CL solution in a simple manner. Exact solutions at relativistic energies for a coaxial cylindrical or concentric spherical diode require numerical integration. The numerical integration can be difficult due to a singularity near the cathode; two methods to overcome the difficulty are presented. Finally, approximate solutions for coaxial cylinder and concentric sphere diodes are presented. The approximate solutions are valid for gap voltages up to 10 MV and for cathode to anode radius ratios from 10^{-5} to 500. The approximate solutions can be used for rapid calculation, and the numerically integrated solutions are employed when high accuracy is needed. One application of this work is the testing of numerical simulation codes that model particle emission, such as particle in cell (PIC) codes.[16] The analytic results discussed herein provide benchmarks for 1D, 2D, and 3D emission algorithms.

ACKNOWLEDGMENTS

The authors acknowledge useful discussions with Don Shiffler and Wilkin Tang. A. D. Greenwood and J. F. Hammond were supported by AFOSR Grant No. 14RD02COR. P. Zhang and Y. Y. Lau were supported by AFOSR Grant No. FA9550-14-1-0309.

[1]C. D. Child, "Discharge from hot CaO," Phys. Rev. **32**, 492 (1911).
[2]I. Langmuir, "The effect of space charge and initial velocities on the potential distribution and thermionic current between parallel plane electrodes," Phys. Rev. **21**, 419 (1923).
[3]I. Langmuir and K. B. Blodgett, "Currents limited by space charge between coaxial cylinders," Phys. Rev. **22**, 347 (1923).
[4]I. Langmuir and K. B. Blodgett, "Currents limited by space charge between concentric spheres," Phys. Rev. **24**, 49 (1924).
[5]E. W. V. Acton, "The space-charge limited flow of charged particles in planar, cylindrical and spherical diodes at relativistic velocities," Int. J. Electron. **3**, 203 (1957).

[6]H. R. Jory and A. W. Trivelpiece, "Exact relativistic solution for the one-dimensional diode," J. Appl. Phys. **40**, 3924 (1969).
[7]Y. Zhang, G. Liu, Z. Yang, Q. Xing, H. Shao, R. Xiao, H. Zhong, and Y. Lin, "Simple solutions for relativistic generalizations of the Child-Langmuir law and the Langmuir-Blodgett law," Phys. Plasmas **16**, 044511 (2009).
[8]X. Chen, J. Dickens, L. L. Hatfield, E.-H. Choi, and M. Kristiansen, "Approximate analytical solutions for the space-charge-limited current in one-dimensional and two-dimensional cylindrical diodes," Phys. Plasmas **11**, 3278 (2004).
[9]V. I. Chetvertkov, "Relativistic characteristics of spherical diodes with radial electron flux," Technical Physics Journal **57**, 93 (1987).
[10]V. M. Belkin, M. A. Zav'yalov, and V. A. Syrovoi, "The limits of the validity of the theory of a spherical diode and the problem of calculation of dense electron beams with substantially different scales," J. Commun. Technol. Electron. **54**, 473 (2009).
[11]Y. B. Zhu, P. Zhang, A. Valfells, L. K. Ang, and Y. Y. Lau, "Novel scaling laws for the Langmuir-Blodgett solutions in cylindrical and spherical diodes," Phys. Rev. Lett. **110**, 265007 (2013).
[12]Y. Y. Lau, "Simple theory for the two-dimensional Child-Langmuir law," Phys. Rev. Lett. **87**, 278301 (2001).
[13]J. W. Luginsland, Y. Y. Lau, R. J. Umstattd, and J. J. Watrous, "Beyond the Child-Langmuir law: A review of recent results on multidimensional space-charge-limited flow," Phys. Plasmas **9**, 2371 (2002).
[14]R. J. Umstattd, C. G. Carr, C. L. Frezen, J. W. Luginsland, and Y. Y. Lau, "A simple derivation of Child-Langmuir space charge limited emission using vacuum capacitance," Am. J. Phys. **73**, 160 (2005).
[15]L. K. Ang and P. Zhang, "Ultrashort-pulse Child-Langmuir law in the quantum and relativistic regimes," Phys. Rev. Lett. **98**, 164802 (2007).
[16]J. J. Petillo, E. M. Nelson, J. F. DeFord, N. J. Dionne, and B. Levush, "Recent developments to the MICHELLE 2-D/3-D electron gun and collector modeling code," IEEE Trans. Electron Devices **52**, 742 (2005).